A.V. NESTEROV, V.S. VASILEVSKY, T.P. KOVALENKO

Bogolyubov Institute for Theoretical Physics, Nat. Acad. of Sci. of Ukraine
(14b, Metrolohichna Str., Kyiv 02680, Ukraine; e-mail: nesterov@bitp.kiev.ua)

PACS 03.65.-w, 03.65.Nk

SPECTRUM OF BOUND STATES OF NUCLEUS ^{10}B IN A THREE-CLUSTER MICROSCOPIC MODEL

In the frame of a microscopic model, namely a three-cluster algebraic version of the resonating-group method, the spectrum of bound states of nucleus ^{10}B *with* $T = 0$ *is considered. As a nucleon-nucleon potential, the semirealistic potential containing the central and spin-orbit components is used. The Coulomb interaction of protons is exactly taken into account. The proper order of levels in the spectrum under study and the reasonable agreement with experimental data on the arrangement of levels relative to the lowest breakup threshold of a nucleus are obtained. The role of the spin-orbit interaction in the formation of the spectrum of bound states of nucleus* ^{10}B *is studied in detail.*

K e y w o r d s: three-cluster model, hyperspherical harmonics, bound states, ^{10}B.

1. Introduction

The purpose of the present work is the study of the spectrum of bound states of nucleus ^{10}B in the frame of a three-cluster microscopic model. This nucleus is odd-odd with $N = Z$, and its spectrum includes the states with the isotopic spins $T = 0$ and $T = 1$. From the viewpoint of the shell model, its structure has the form $(1s)^4(1p3/2)^6$. The total angular momentum of the ground state is equal to $J = 3$, which is explained by peculiarities of the filling of the p-shell. The SU(3)-multiplet of the basic configuration has quantum numbers (Elliott's indices) $(\lambda, \mu) = (2, 2)$ consistent with the following values of total orbital momentum: $L^\pi = 0^+$, 2^+, 2^+, 3^+, and 4^+, where the state 2^+ is met twice at the reduction of SU(3) onto O(3). Though the model used in the present work is much more general than the oscillator shell model in its lowest configuration, we may expect, however, that the former contains the mentioned states in the low-energy region of excitations of nucleus ^{10}B, where the experiment shows the presence of bound states, whose number is unconventionally large for a nucleus of the p-shell. The last circumstance was, in particular, one of the stimuli to separate the consideration of the spectrum of bound states of nucleus ^{10}B as an independent problem.

To explain our interest in this question, we consider its modern theoretical state. In order to clarify the present situation, we will analyze the results of previous calculations, which are called the *ab initio* calculations made, in particular, in the frame of the no-core shell model (NCSM), which becomes popular with the appearance of supercomputers. These results are, in our opinion, the most demonstrative at the present time. The mentioned model called else the shell model without inert core uses the oscillator basis of the shell model and considers all nucleons to be spectroscopically active. In this case, the calculations usually involve a huge number ($\approx 10^8$) of basis functions, and the nucleon-nucleon interaction is modeled by potentials based on the ideas of the meson exchange or on the reasoning considering the quark structure of nucleons in the frame of the chiral effective field theory.

On the initial stage, the similar calculations were carried out with the realistic nucleon-nucleon potentials CD-Bonn and Argonne v'_8 [1–3]. In the first work, it was obtained that the ground state is 1^+, whereas the experiment shows that it is the 3^+-state lying by 0.72 MeV lower than the 1^+-state. It is worth noting that the nucleon-nucleon potential in the second and third works contained effective three-particle forces, whose significance was indicated by the authors. But the hope for that these forces will correct completely the situation with the inversion of levels was not realized on the great score.

While setting the nucleon-nucleon forces, the authors of work [4] used the potential N3LO (next-to-next-to next-to-leading order) obtained in the fourth order of the chiral perturbation theory without regard for three-particle forces. The inversion of the

3^+- and 1^+-levels was obtained again, and this result was commented to be due to the neglect of three-particle forces. The calculations with N2LO three-particle forces, which required a very high loading of supercomputers, in two somewhat different modifications of the NNN potentials led to the questionable success [5].

In the previous work [6], the fitting of the low-energy constants in contact NNN terms of the potential in view of the binding energy of nuclei with $A = 3$ was performed. The obtained results including, in particular, the spectrum of nucleus ^{10}B led the authors to the conclusion about the necessity of a further improvement of the chiral Hamiltonian. The inversion of levels of nucleus ^{10}B, which was obtained in the majority of cases, forced the authors of work [5] to claim that the description of the spectrum of bound states of this nucleus is a true challenge to all *ab initio* calculations.

We add that the similar difficulties are characteristic of the calculations in [7] on the basis of NCSM with the use of NN-forces in JISP16 (J-matrix inverse scattering potential 16), which were obtained within the J-matrix method of inverse scattering transform with the use of a fitting to nucleon-nucleon data. This concerns also the results in [8], where the quantum Monte-Carlo method was used with the application of the potential Argonne v_{18} and the potentials of three-particle forces of the Urbana IX and Illinois types as three-nucleon potentials. The proper order of the above-mentioned levels was obtained in the last case. These results supplement the above-presented uncertain situation concerning the spectrum of bound states of nucleus ^{10}B as a result of the *ab initio* calculations and some simpler approaches such as, for example, the method of random phases and indicate that the question requires a more profound consideration.

Before the above-mentioned calculations, the spectrum of nucleus ^{10}B was considered in [9] in the frame of the multiconfiguration multichannel resonating-group method. There, the Minnesota potential [10] was used. Its parameters were fitted by the low-energy nucleon-nucleon scattering data, and the model space contained the binary channels $\alpha + {}^6$Li, $d + {}^8$Be, $\alpha + {}^6$Li*, and $d + {}^8$Be*, where the asterisks denote the excited states of nuclei with $L = 2$. In view of the last circumstance, the attempt to approximately account for the three-cluster structure $\alpha + \alpha + d$ was made. The Coulomb repulsion of protons was not considered. But the main shortcoming of the mentioned calculations consisted in that, from our viewpoint, the spin-orbit forces (LS-forces) were not taken into account in them. The estimation of the spin-orbit splitting was obtained on the basis of the results in [11], where the spectrum of nucleus ^{10}B was considered in the frame of the three-cluster model with the approximate account for the Pauli principle by the method of orthogonalization conditions. The calculations were performed with the Hasegawa–Nagata potential. In this case, it was indicated in [9] that the proper mutual position of the levels was obtained.

In the present work, the spectrum of bound states of nucleus ^{10}B is considered in the frame of a three-cluster variant of the algebraic version of RGM (AV RGM) (see, e.g., [12,13]) with the use of a hyperspherical oscillator basis. In this model, the Pauli principle is exactly taken into account. To model nucleus ^{10}B as a three-cluster system, we choose the configuration $\alpha+\alpha+d$, for which the three-cluster threshold energy is minimal among all possible three-cluster configurations. With its help, we can consider the dominating binary channel $\alpha + {}^6$Li, which defines mainly, as we can boldly assume, the properties of bound states and a number of resonances related to nucleus ^{10}B. It is worth noting that the three-cluster configuration $\alpha + \alpha + d$ describes the states of a compound-nucleus with the total spin $S = 1$ and the isospin $T = 0$. (It is of interest that the existence of the indicated cluster configuration as a leading one is indirectly confirmed not only by the general reasoning, but by the experimental results obtained on a nucleotron [14].)

In the numerical calculations of the spectrum of ^{10}B, we used, similarly to [9], the semirealistic Minnesota potential [10], which describes reasonably the properties of nuclei of the s-shell and the LS-forces in version IV in [15]. The latter have a simple form represented by a single term, which allows us to sufficiently easily consider the dependence of the obtained results on the intensity of these forces. The parameters of LS-forces were fitted by the phase shifts for $\alpha + n$ and $\alpha + p$ scattering at low energies Here, we took the Coulomb interaction of protons into account as well.

We accept the following plan. We present the main ideas of the used theoretical approach in Section 2 and the results of its application to the description

of characteristics of the spectrum of bound states of nucleus ^{10}B in Section 3.

2. Method

By presenting AV RGM in its three-cluster variant, we start from a three-cluster ansatz of the traditional version of RGM [16]. RGM seems to be one of the most successive and efficient tools to study the dynamics of cluster configurations in light atomic nuclei. In this case, the completely antisymmetrized multiparticle wave function of a three-cluster nuclear system consisting of A nucleons with the clusterization $A = A_1 + A_2 + A_3$ can be set, in the frame of RGM, as

$$\Psi_J(\mathbf{q}_1, \mathbf{q}_2, ..., \mathbf{q}_{A-1}) = \\ = \sum_{L,S} \widehat{\mathcal{A}}\big\{[\Psi_1(A_1)\,\Psi_2(A_2)\,\Psi_3(A_3)]_S \times \\ \times \Psi_{LS;J}(\mathbf{q}_1, \mathbf{q}_2)\big\}_J, \quad (1)$$

where $\widehat{\mathcal{A}}$ is the operator of antisymmetrization, and $\Psi_i(A_i)$ is the function describing the internal structure of the i-th cluster. The functions $\Psi_i(A_i)$ are fixed from the onset, which corresponds to the use of the approximation of "frozen" nucleon distribution densities for the clusters. As usual, we choose these functions as those of a multiparticle spherically symmetric shell model with the most compact filling of shells. The function $\Psi_{LS;J}(\mathbf{q}_1, \mathbf{q}_2)$ depends on the Jacobi coordinates setting the mutual position of the clusters and must be determined by solving some equation following from the Schrödinger equation and by setting the required function in the form (1).

In the definition of the antisymmetric function $\Psi_i(A_i)$ of the i-th cluster, we omit, for simplicity, two significant quantities: the spin S_i of a cluster and the oscillator radius (the oscillator length) b. Since the wave function $\Psi_i(A_i)$ is constructed, as was mentioned above, from one-particle functions of the multiparticle shell model, it depends explicitly on the oscillator length b. In this approach, b is a fitting (variational) parameter, whose choice will be discussed in Section 3. We now consider the spin of a cluster. As was clearly indicated in Eq. (1), we use the LS-scheme of coupling of the orbital and spin momenta for the classification of states of the three-cluster system. In this scheme, the total spin S of the system is defined as the vector sum of the spins of individual clusters: $\mathbf{S} = \mathbf{S}_1 + \mathbf{S}_2 + \mathbf{S}_3$. The total angular momentum $\mathbf{J}$ of the system is, in turn, the vector sum of the total orbital momentum $\mathbf{L}$ and the total spin $\mathbf{S}$ of the compound-nucleus: $\mathbf{J} = \mathbf{L} + \mathbf{S}$.

The undoubtful advantages of the resonating-group method consist in the following: (i) it is a microscopic approach, in which the dynamics of clusters is defined by the nucleon-nucleon interaction, (ii) the Pauli principle is taken into account explicitly, and (iii) the motion of the center of masses is separated in the explicit form. The second item is especially significant for the consideration of bound states and states of the continuous spectrum of light nuclei at comparatively small energies. RGM, as one of the most successive realizations of the cluster model, allows one to properly consider the boundary conditions and to perform a theoretical analysis of results with regard for those physical properties of the systems under study, which seem to be the most important in each specific case.

There exist several alternative versions of the resonating-group method. They differ from one another by the procedures of solution of the equations for the determination of the spectrum of bound states and the parameters of elastic and inelastic scattering. Many versions of RGM involve different discrete schemes for the numerical solution of dynamical equations. One of the popular trends in the realization of these schemes is the use of square-integrable bases of functions. As a rule, the basis functions are attracted for the description of only the internal part of the wave function, and the asymptotic part is determined in the coordinate representation. In AV RGM, the discrete scheme is realized with the help of an orthonormalized set of oscillator functions. As distinct from the alternative versions of RGM, these functions describe both the internal and asymptotic parts of the wave function. In essence, AV RGM is the self-consistent matrix form of quantum mechanics for a multiparticle system, for which the wave function and the boundary conditions are defined in a discrete space.

In correspondence with the above discussion, the wave function $\Psi_{LS;J}$ can be represented as follows:

$$\Psi_{LS;J}(\mathbf{q}_1, \mathbf{q}_2) = \sum_{\nu} C_{\nu;LS;J} |\nu\rangle_F. \quad (2)$$

Here, the aggregate index ν is a set of six quantum numbers characterizing the wave functions of the total basis $|\nu\rangle_F = |\nu; \mathbf{q}_1, \mathbf{q}_2\rangle_F$ chosen by us, i.e., the

F-representation, by which we make transition, in fact, to the matrix representation of quantum mechanics. The functions $|\nu\rangle_F$ are the principal component for the construction of three-cluster antisymmetric oscillator functions

$$|\nu\rangle = \widehat{\mathcal{A}}\{\Psi_1(A_1)\Psi_2(A_2)\Psi_3(A_3)|\nu;\mathbf{q}_1,\mathbf{q}_2\rangle_F\}. \quad (3)$$

The set of antisymmetric oscillator functions (3) is used for the expansion of the three-cluster function (1):

$$\Psi_J = \sum_\nu C_{\nu;LS;J}|\nu\rangle. \quad (4)$$

Thus, we have to determine the set of coefficients $\{C_{\nu;LS;J}\}$. In view of Eq. (1), this set defines, in fact, the multiparticle wave function of the nucleus under consideration and must be determined by solving of the Schrödinger equation in the matrix form, i.e., a system of linear algebraic equations of the form

$$\sum_{\widetilde{\nu}}\left[\left\langle\nu\left|\widehat{H}\right|\widetilde{\nu}\right\rangle - E\langle\nu|\widetilde{\nu}\rangle\right]C_{\widetilde{\nu}} = 0, \quad (5)$$

where $\left\langle\nu\left|\widehat{H}\right|\widetilde{\nu}\right\rangle$ and $\langle\nu|\widetilde{\nu}\rangle$ are matrix elements of the Hamiltonian and the identity operator between antisymmetrized multiparticle basis functions.

As the total basis for the expansion of the relative-motion function, we will use the basis of a six-dimensional spherically symmetric harmonic oscillator. In this case, the matrix of the operator of kinetic energy has a convenient three-diagonal (Jacobi) form. In other words, we use, in fact, the approach called the method of J-matrix [17, 18]. For the basis of a six-dimensional harmonic oscillator, we may use various schemes of classification of functions. For example, three such possibilities related to the reduction of the unitary group $U(6)$, which is a symmetry group for a six-dimensional harmonic oscillator, onto its subgroups were considered in [13, 19]. In the present work, we choose the scheme

$$U(6) \supset O(6) \supset SO(3)\otimes SO(3) \supset SO(3). \quad (6)$$

This gives us the following quantum numbers: the hypermomentum K, number of quanta of hyperradial excitations n_ρ, partial angular momentum l_1 related to the first Jacobi vector, partial angular momentum l_2 related to the second Jacobi vector, and L and M that are the momentum obtained by the coupling of the partial momenta l_1 and l_2 and its projection M, respectively. Thus, we work with hyperspherical harmonics [20, 21] on a six-dimensional sphere, and our basis functions in the below-indicated variables take the form

$$|\nu\rangle = |n_\rho, K, l_1, l_2; LM\rangle =$$

$$= \mathcal{N}_{NK}\exp\left\{-\frac{1}{2}\rho^2\right\}\rho^K L_{n_\rho}^{K+2}\left(\rho^2\right)\Phi_K^{l_1,l_2;L}(\Omega), \quad (7)$$

where $\mathcal{N}_{NK}$ is the normalizing factor, ρ is the hyperradius ($\rho^2 = \mathbf{q}_1^2 + \mathbf{q}_2^2$), which defines the sizes of the system and is related to the quantum number n_ρ, $L_{n_\rho}^{K+2}\left(\rho^2\right)$ is the generalized Laguerre polynomial, and $\Phi_K^{l_1,l_2;L}(\Omega)$ is a hyperspherical harmonic depending on five hyperangles: $\beta, \theta_1, \phi_1, \theta_2$, and ϕ_2. Here, the first angle can be given by the relation $\beta = \arctan(|\mathbf{q}_1|/|\mathbf{q}_2|)$, defines the shape of a triangle formed by clusters, and is related to the quantum number K. Four remaining angles set pairwise determine the directions in the space of vectors $\mathbf{q}_1$ and $\mathbf{q}_2$, respectively. For the sake of definiteness, we consider here and below that the vector $\mathbf{q}_1$ joins the center of masses of the subsystem $\alpha-\alpha$ with the center of masses of the deuteron cluster, and $\mathbf{q}_2$ joins the centers of masses of the α clusters.

Having determined completely the full basis needed in what follows, it is necessary to make the next step and to calculate matrix elements of the Hamiltonian $\langle\nu|\widehat{H}|\widetilde{\nu}\rangle$ and the overlap integral $\langle\nu|\widetilde{\nu}\rangle$. The direct calculation of the mentioned matrix elements between the basis functions (7) is a very complicated technical task. This forced developing a special calculation technique for calculating the required quantities. It is based on the use of the generating functions and the generating matrix elements, which allows one to obtain the recurrence relations for all matrix elements of interest. Since this task is a separate item, whose discussion will require a large place for bulky formulas, we mention works [12, 22], where this technique of calculations is presented sufficiently completely.

By this, we could finish the description of the used approach in the frame of AV RGM. But we note else that this approach is, at the present time, a completed specific realization of matrix quantum mechanics with proper boundary conditions for states of the discrete and continuous spectra. In particular, the asymptotic

formulas describing a large number of radial excitations were obtained for components of a wave function in the oscillator representation [23–27]. In other words, whereas the solution of problems for the discrete or continuous spectrum uses usually the asymptotic formula for a wave function at large distances in order to set the boundary conditions in the coordinate representation, the practically equivalent procedure is realized in the oscillator representation. For the large numbers of radial oscillator quanta of the relative motion of clusters, we consider the asymptotic formulas, but already for the coefficients of an expansion of the relative-motion function.

There is one more question needed to be considered. It consists in that, as was indicated above, the Pauli principle is taken into account exactly in the present approach, and it is necessary to exclude the Pauli forbidden states. As is known, the problem consists in the following. The basis functions $|\nu\rangle_F$ are orthonormalized. But at the same time, the operator of antisymmetrization participating in the construction of the antisymmetric oscillator functions (4) breaks the orthogonality and the normalization of the functions $|\nu\rangle$. Moreover, the operator of antisymmetrization causes the appearance of linearly dependent functions, which correspond to the Pauli forbidden states. Here, they are excluded by means of the diagonalization of the antisymmetrization operator matrix $\|\langle\nu|\widetilde{\nu}\rangle\| = \|\langle\nu|\widehat{\mathcal{A}}|\widetilde{\nu}\rangle\|$, which is calculated on the multiparticle basis functions, and by omitting to the eigenvectors of the matrix $\|\langle\nu|\widetilde{\nu}\rangle\|$ with zero eigenvalues. As for the allowed states that are eigenfunctions of the antisymmetrizator, they can be constructed in the form of linear combinations of the input basis functions of the given oscillator shell. The last circumstance is related to the fact that the matrix $\|\langle\nu|\widetilde{\nu}\rangle\|$ has a block structure, and its nonzero matrix elements arise at the overlapping of functions that belong to the same oscillator shell and satisfy the condition $N = \widetilde{N}$. After the elimination of the forbidden states, our system of equations (5) takes a somewhat different form. If $\|U_{\alpha,\nu}\|$ is the matrix of eigenvectors of the operator of antisymmetrization, we obtain

$$\sum_{\widetilde{\alpha}} \left[\langle\alpha|\widehat{H}|\widetilde{\alpha}\rangle - E\delta_{\alpha,\widetilde{\alpha}}\right] C_{\widetilde{\alpha}} = 0, \tag{8}$$

where $\|\langle\alpha|\widehat{H}|\widetilde{\alpha}\rangle\|$ is the Hamiltonian matrix calculated already on such linear combinations of the input multiparticle basis functions, which correspond to the Pauli allowed states. In this case, the new matrix of the Hamilton operator is connected with the matrix $\|\langle\nu|\widehat{H}|\widetilde{\nu}\rangle\|$ by the relation

$$\langle\alpha|\widehat{H}|\widetilde{\alpha}\rangle = \sum_{\nu,\widetilde{\nu}} U_{\alpha,\nu}\langle\nu|\widehat{H}|\widetilde{\nu}\rangle U_{\widetilde{\alpha},\widetilde{\nu}}.$$

In our approach, the system of linear algebraic equations (8) describes completely the dynamics of the three-cluster system under study with regard for the Pauli principle, and its solutions determine uniquely the spectrum and the wave functions of bound states or the wave functions and elements of the scattering matrix for states of the continuous spectrum.

3. Discussion of Results

As was mentioned above, we consider the spectrum of bound states of nucleus ^{10}B in the three-cluster representation $\alpha + \alpha + d$. Since the spin of an α particle is zero, the total spin S of the system is determined by the spin of a deuteron and, therefore, is equal to 1. This implies that the state with the total angular momentum J must consist of states, in which the total orbital momentum L takes the values $L = J - 1$, $L = J$, and $L = J + 1$. For example, the total orbital momentum $J^\pi = 3^+$ can be obtained with the use of the angular momenta $L = 2$, 3, 4, and the states $J^\pi = 1^+$ are states with $L = 0$, 1, 2, and so on. This means that the wave function (1) can be represented as a vector consisting of three components $\Psi = \{\Psi_{L=J-1}, \Psi_{L=J}, \text{ and } \Psi_{L=J+1}\}$, and the Schrödinger equation can be conditionally presented in a block form

$$\left\| \begin{array}{ccc} (\widehat{H}_C + \widehat{V}_{\rm LS})_{J-1,J-1} & (\widehat{V}_{\rm LS})_{J,J-1} & 0 \\ (\widehat{V}_{\rm LS})_{J,J-1} & (\widehat{H}_C + \widehat{V}_{\rm LS})_{J,J} & (\widehat{V}_{\rm LS})_{J-1,J+1} \\ 0 & (\widehat{V}_{\rm LS})_{J+1,J} & (\widehat{H}_C + \widehat{V}_{\rm LS})_{J+1,J+1} \end{array} \right\| \left\| \begin{array}{c} \Psi_{J-1} \\ \Psi_J \\ \Psi_{J+1} \end{array} \right\| = E \left\| \begin{array}{c} \Psi_{J-1} \\ \Psi_J \\ \Psi_{J+1} \end{array} \right\|, \tag{9}$$

where $\widehat{H}_C = \widehat{T} + \widehat{V}_{NN} + \widehat{V}_C$ is the central part of the Hamiltonian consisting of the operator of kinetic energy, central part of the nucleon-nucleon potential, and Coulomb potential, respectively, and $\widehat{V}_{\rm LS}$ is the potential of spin-orbit forces.

In order to describe the spectrum of bound states of nucleus ^{10}B , we chose the Minnesota potential as the nucleon-nucleon potential. Then we obtained the exchange parameter as a free parameter (Majorana parameter) of the potential in addition to the oscillator radius b, whose value is taken here to be the same in the construction of the wave functions of all clusters. The former is connected with the amplitudes of odd components, which are mainly responsible for the repulsion of nucleons at small distances. Both parameters should be determined from the physical reasoning prior to the solution of the system of equations (9).

Here, we consider three possible means to set the free parameters. They correspond to three different choices of the nucleon distribution densities in clusters and, respectively, to three different effective potentials of interaction of clusters. In the first case (C1), we choose a value of oscillator radius that minimizes the energy of the three-cluster threshold $\alpha + \alpha + d$ and take u such that it ensures the proper position of the ground state of nucleus ^{10}B relative to the indicated threshold. In case (C2), we choose a value of b, at which the binary threshold $\alpha + d$ in nucleus ^{6}Li has the minimal energy, and u ensures the proper position of the ground state ^{6}Li relative to the threshold of $\alpha + d$. In the third case (C3), the parameter u is chosen as in (C2), and b was determined from the condition of the best description of the root-mean-square radius of an α particle. In other words, choice (C3) is the same as in [9]. The distinction consists in that we take both the spin-orbit interaction and the Coulomb potential into account in the present work. For reader's convenience, we give the values and the means of choice of the input parameters of the model in Table 1.

Table 1. **Versions of the choice of the input parameters b and u of the problem**

Version of calculations	C1	C2	C3
b, fm	1.298	1.3110	1.39482
u	0.900	0.9254	0.9070
Optimization	$\alpha + \alpha + d$	$\alpha + d$	α
Fitting	^{10}B	^{6}Li	^{6}Li

Table 2. **Results of calculations of the spectrum of bound states of nucleus ^{10}B for various collections of the parameters u and b. The energies are reckoned from the lowest breakup threshold of nucleus ^{10}B, which is the threshold $^6\mathrm{Li} + \alpha$**

Quantum numbers	Exp.	Theory		
		C1	C2	C3
J^π	E, keV	E, keV	E, keV	E, keV
3^+	-4459.60	-5130.20	-6993.55	-4583.37
1^+	-3741.22	-3802.13	-4942.66	-4058.54
1^+	-2305.33	-893.33	-2497.70	-1429.39
2^+	-872.47	40.03	-1348.23	-542.02

The results of calculations of the spectrum of bound states with $S = 1$ and $T = 0$ of nucleus ^{10}B for three collections of parameters b and u given in Table 1 are presented in Table 2, where the first column gives experimental data from work [28]. It is worth noting that, on the given stage, we vary only the mixing parameter u related to the central part of the nucleon-nucleon potential. In the calculations, we used the values of parameters of LS-forces, which were recommended in work [15]. The dependence of the results of calculations on the intensity of spin-orbit forces will be considered below in detail. In our calculations, we take all basis functions with hypermoments up to $K_{\max} = 14$ and with the radial quantum number n_ρ up to 100, which ensures the quite reasonable convergence of the results.

In a more descriptive form, the results of Table 2 are presented in Fig. 1, where we omitted, like that in the table, the level with the quantum numbers $J^\pi = 0^+$ and with the isotopic spin equal to 1. In order to describe this level, it is necessary to consider the four-cluster configuration $\alpha + \alpha + p + n$.

The comparison of the results of calculations with experimental data indicates in the first turn that we obtained the proper positions of the levels. As for their mutual arrangement, variant (C3) seems to be the most successful. Apparently, it is not accident that just such means to set the parameters was used in work [9], though the choice of parameters was not discussed there. In what follows, we present only those theoretical results that were ob-

tained with the use of the collection of parameters (C3).

In the first part of this work, we paid a sufficiently significant attention to the discussion of the results of calculations performed in the no-core shell model. Now, we present the most representative results from work [5] in order to compare them with our results in Fig. 2. In this case, we took only the levels with $T = 0$ and remained only one of three versions of calculations of the NCSM2 type differing by the values of oscillator radius. In our opinion, the chosen version describes utmost adequately the experimental situation. The results in [5] were obtained with the use of modern two- and three-nucleon chiral interactions (chiral effective field theory (EFT) of two- and three-nucleon interactions). For example, the calculations of the NCSM3 type were performed, by using the N3LO NN forces. Those results suffer from the same drawbacks, as the results of calculations with realistic potentials, which were mentioned in Introduction. We note that the proper value of total momentum in the ground state can be obtained only with the potential N2LO NNN with the energy cutoff at 500 MeV (NCSM2). It is worth noting that a weaker chiral N2LO NNN NCSM1 potential with the NNN energy cutoff at 400 MeV led again to the inversion of the 1^+ and 3^+ states.

At the beginning of this section, we mentioned how the states with definite values of total angular momentum J can be obtained from the states with different values of total orbital momentum L. The results of consideration of the question about the contribution of states with the admissible values of L to a state with some value of J are given in Table 3 for various specific cases.

As is seen from the results presented in Table 3, the wave function of the ground state shows the most remarkable distribution over states with a total orbital momentum. Of course, the leading role in this case is played by the states with $L^\pi = 2^+$, but the state with $L^\pi = 3^+$ gives a sufficiently significant contribution. As for the contribution of the state with $L^\pi = 4^+$, it equals about 1.5%. For the $J^\pi = 1^+$ states, the situation is somewhat different. The first and the second states are formed practically completely from states with the total orbital momenta 0^+ and 2^+, respectively. The wave function of the state with $J^\pi = 2^+$, like the second 1^+-state, consists mostly of the wave function with $L^\pi = 2^+$ and the 3-% admixture of the wave function with $L^\pi = 3^+$. Thus, the states with anomalous parity, as distinct from the states with normal parity, take no noticeable participation in the formation of the spectrum

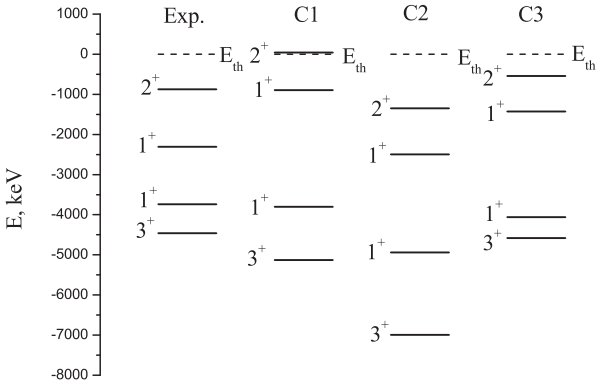

Fig. 1. Spectra of bound states of nucleus ^{10}B with $T = 0$ obtained with the use of the collections of input parameters C1, C2, and C3 (see Table 1). In each case, the quantity $E_{\rm th}$ is the $^6{\rm Li}+\alpha$ threshold energy for nucleus ^{10}B; all other energies are reckoned from it

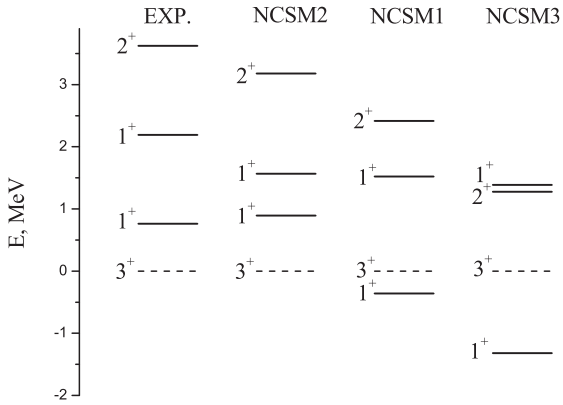

Fig. 2. Spectra of bound states of nucleus ^{10}B with $T = 0$ obtained in [5] with the use of two- and three-nucleon chiral interactions (see the text). All energies are reckoned from the energy of the 3^+ state

Table 3. **Weights $W(L)$ of states with the various values of angular momentum in the wave function of the bound J^π-state of nucleus ^{10}B given in per cent**

J^π	E, keV	$L=0$	$L=1$	$L=2$	$L=3$	$L=4$
3^+	-4583			83.64	14.92	1.44
1^+	-4059	99.92	0.07	0.005		
1^+	-1429	0.003	0.001	99.99		
2^+	-542		0.01	96.91	3.08	

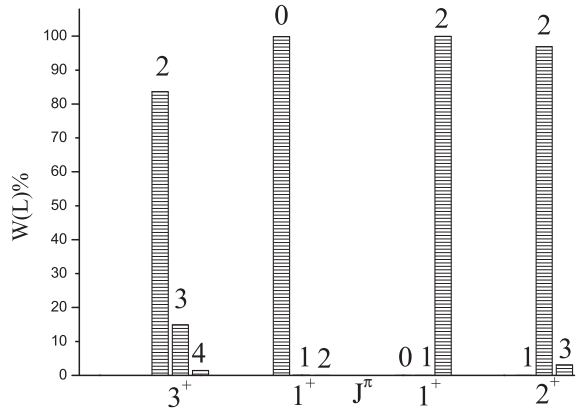

Fig. 3. Contributions of states with the various values of angular momentum to the wave functions of bound states of nucleus ^{10}B with $T = 0$ (see the text)

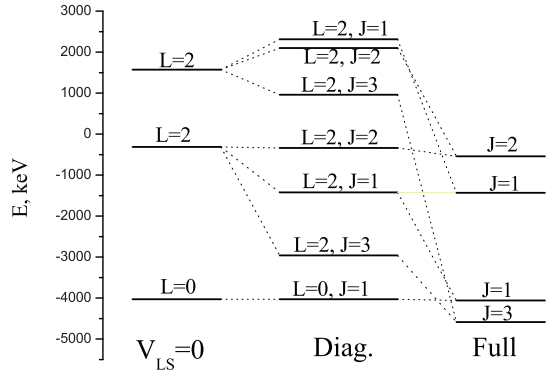

Fig. 4. Spectra of bound states of nucleus ^{10}B obtained in the $\widehat{V}_{\rm LS} = 0$ and "diagonal" approximations, as well as in the complete proper calculation (Full)

of excited states. Undoubtedly, this defines the mutual position of the levels in many aspects.

The visualization of the data from Table 3 is realized in Fig. 3. It is a histogram, where each of four groups of columns (three in each group) corresponds to a state with the definite values of total angular momentum J and parity π, and each of the columns demonstrates the contribution $W(L)$ of a function with some value of total orbital momentum to this state. The values of total orbital momenta are given by numbers above each of the columns.

To understand the role of the spin-orbit interaction in the formation of bound states of ^{10}B, we made two additional calculations. First, we switched off the spin-orbit interaction. This calculation will be referred as $\widehat{V}_{\rm LS} = 0$. In this case, the Hamiltonian contains only central forces, and, thus, the total orbital momentum L is a quantum number. Second, the spectrum of ^{10}B was obtained in the diagonal approximation. These results will be called "diagonal". The diagonal approximation is realized by omitting the off-diagonal matrix elements of the spin-orbit interaction in the system of equations (9) or, in other words, by assuming that $(\widehat{V}_{\rm LS})_{L,\widetilde{L}} = 0$, when $L \neq \widetilde{L}$. In this case, the spin-orbit interaction takes part in the formation of the spectrum of bound states. However, both the total angular momentum J and the total orbital momentum L are integrals of motion. When we transit from $\widehat{V}_{\rm LS} = 0$ to "diagonal" calculations, we observe that the spin-orbit interaction splits the state with the total orbital momentum L into three states with the different values of total angular momentum J: $J = L - 1$, $J = L$, and $J = L + 1$. One exception of this rule is the state with the total orbital momentum $L = 0$, where the spin-orbit interaction has zero contribution, and only one state with $J = 1$ is emerged. Thus, each state in the "diagonal" calculation has to be marked by two quantum numbers L and J. In Fig. 4, one can compare the results obtained with $\widehat{V}_{\rm LS} = 0$ and in the "diagonal" approximation. In this figure, we also display the correct solution of Eqs. (9), which is marked as Full. In the Full calculation, the energy levels are obtained in the "diagonal" approximation with a fixed value of total angular momentum J, but the different values of total orbital momentum L.

The wave function of an eigenstate of Hamiltonian (9) obtained in the Full calculation is a combination of wave functions determined in the "diagonal" approximation with the fixed value of total angular momentum, but with the different values of total orbital momentum. The contribution of different orbital L states to the states with the total angular momentum J is determined by the off-diagonal matrix elements of the spin-orbit interaction $(\widehat{V}_{\rm LS})_{L,\widetilde{L}}$.

One can see that there are some energy levels with the same energy in the $\widehat{V}_{\rm LS} = 0$ and "diagonal" approximations. This means that the spin-orbit interaction has small effects on these levels. They are the $L = 0$ and $L = 0$, $J = 1$ states, where, as was pointed above, the spin-orbit interaction has zero contributions, and the $L = 2$ and $L = 2$, $J = 2$ states in the $\widehat{V}_{\rm LS} = 0$ and "diagonal" approximations, respectively. The later situation needs some additional consideration. If the spin-orbit interaction is a small per-

turbation, then the splitting energy arising from this interaction would be determined by the well-known formula

$$\Delta E_{LJ} \approx \frac{1}{2}[J(J+1) - L(L+1) - S(S+1)]\overline{(V_{\rm LS})}_L,$$

where $\overline{(V_{\rm LS})}_L$ is the expectation value of spin-orbit interaction in the unperturbed state with the total orbital momentum L. In our case, the total spin $S = 1$. Therefore, for $L = 2$, we obtain the energy shift as

$$\Delta E_{LJ} = \overline{(V_{\rm LS})}_L \begin{cases} 2, & J = 3, \\ -1, & J = 2, \\ -3, & J = 1. \end{cases}$$

If $\overline{(V_{\rm LS})}_L$ is negative, then the state with $J = 3$ moves down, and the states with $J = 2$ and $J = 1$ move up. According to this rule, the state with the total angular momentum $J = 2$ should be lower in energy than the state with $J = 1$. Both have to lie above the unperturbed $L = 2$ state (i.e., in the $\widehat{V}_{\rm LS} = 0$ approximation). We see that such splitting of states is observed for the second state with $L = 2$. However, the order of the $J = 2$ and $J = 1$ states contradicts the rule. This means that the perturbation method is not totally valid for this $L = 2$ state.

As for the first state with the total orbital momentum $L = 2$, it also does not obey the perturbation method. However, the order of states with the total angular momentum J is in accordance with the above-mentioned rule. But all three states ($J = 3$, $J = 2$, and $J = 1$) are below the unperturbed $L = 2$ state. This indicates that, in the "diagonal" calculations, the expectation value $\overline{(V_{\rm LS})}_L$ depends not only on the total orbital momentum L, but also on the total angular momentum J.

In the same manner as in the approach with linear Hermitian operators, we can calculate the quantum-mechanical means of various quantities in the frame of matrix quantum mechanics. First, we consider $\left\langle J^\pi \left| \mathbf{q}_1^2 \right| J^\pi \right\rangle$ and $\left\langle J^\pi \left| \mathbf{q}_2^2 \right| J^\pi \right\rangle$. This gives us possibility to determine an average isosceles triangle formed by clusters on a plane for each of the states of a discrete spectrum. The results are presented in Table 4, where $r\,(\alpha - \alpha)$ stands for the average distance between the α-clusters, i.e., the length of the triangle base. The height of the triangle is $r\,(d - \alpha\alpha)$, which is the average distance between the center of masses of two α clusters and the deuteron cluster. In the same table, we show the value of proton root-mean-square radius R_p for each of the states, whose value in our model coincides with the values of neutron and mass radii.

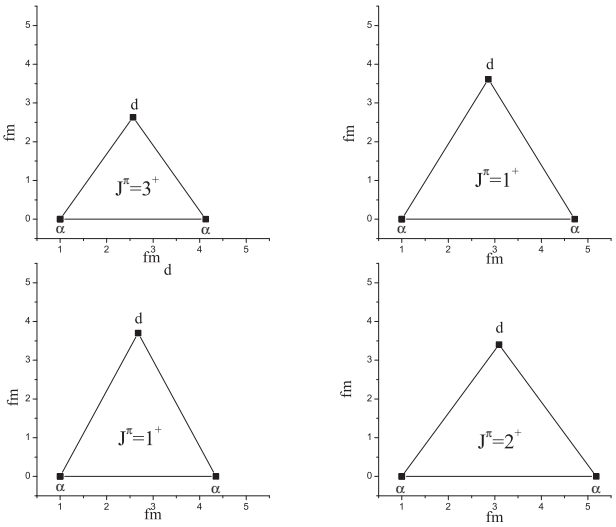

Fig. 5. Triangles representing the averaged mutual position of clusters for the bound states of nucleus ^{10}B with $T = 0$

For the better clearness, the triangles formed by clusters are presented in Fig. 5.

As follows from the results presented in Table 4 and in Fig. 5, nucleus ^{10}B has the most compact configuration in the ground state. For this state, the experimental value of proton root-mean-square radius is available and is equal to 2.30 ± 0.12 fm [29], which agrees well, with regard for experimental errors, with the theoretical value of 2.23 fm obtained by us. It is worth noting that, for example, the no-core shell model with the use of the NN and NN + NNN forces following from the effective chiral field theory gives the values of 2.256 fm and 2.197 fm, respectively, for the root-mean-square radius (see, e.g., [6]). In other words, the three-particle forces, which are used in the *ab initio* calculations in order to correct the situation with the order of the positions of levels, contract the

Table 4. **Mean values of parameters of the triangles formed by clusters for the bound states of nucleus ^{10}B and their proton root-mean-square radii**

Radius, fm	$J^\pi = 3^+$	$J^\pi = 1^+$	$J^\pi = 1^+$	$J^\pi = 2^+$
$r\,(d - \alpha\alpha)$	2.630	3.612	3.693	3.369
$r\,(\alpha - \alpha)$	3.132	3.709	3.252	4.138
R_p	2.229	2.502	2.398	2.539

system. It seems to us that the relative compactness of the nucleus in the ground state in our case is ensured by a sufficiently strong spin-orbit interaction.

Apparently, it is more convenient to use not only the language of a hyperspherical basis, which we used in calculations, but also that of a bioscillator basis (see, e.g., [12, 13]), whose functions are classified by the quantum numbers n_1, l_1, n_2, l_2; LM. Here, n_1 is the number of oscillator quanta of the excitation along the Jacobi vector $\mathbf{q}_1$, which is associated with the heights of triangles in our case, l_1 is the partial momentum related to the Jacobi vector, n_2 is the number of oscillator quanta of the excitation along the Jacobi vector $\mathbf{q}_2$, which is associated with the bases of triangles, and l_2 is the partial momentum related to the second Jacobi vector. In this case, n_2 and, respectively, l_2 take only the even values due to the symmetry of the $\alpha - \alpha$ subsystem. In our case as a result of the action of the Pauli principle, $n_{2_{\min}} = 4$ and, respectively, $n_{1_{\min}} = 2$, since $N_{\min} = 6$, and $N = n_1 + n_2 = K + 2n_\rho$ in all cases.

It is natural that, in the frame of the same oscillator shell with the given value of principal quantum number, the functions of the mentioned bases are connected by a unitary transformation as the eigenfunctions of the same Hamiltonian of a six-dimensional harmonic oscillator presented in different variables. In other words, the function of one basis is a linear combination of functions of another basis on the given shell.

Both triangles in Fig. 5 corresponding to the states 1^+ have larger sizes, as compared with the case of the states 3^+, and noticeably different shapes. The first triangle (above on the right) has a larger base than the second one (below on the left), but its height is less. The triangle for the first 1^+ state has a more regular shape due to, apparently, that this state is formed almost completely from the wave function with the total orbital momentum $L = 0$ and, hence, mainly from states with the partial momenta $l_1 = l_2 = 0$ ($K = 0$). The last assertion must be true by virtue of the commonly known fact that the interaction of nucleons is manifested most strongly namely in the s-state, and it is completely confirmed by our entire experience of three-cluster calculations. The second $J^\pi = 1^+$ state is formed practically by 100% from the states with $L = 2$ and, hence, mainly from the basis functions with the partial orbital momenta $(l_1, l_2) = (2, 0), (0, 2)$. Moreover, the large role is played namely by the first state and, generally, by the basis functions corresponding to excitations along the vector $\mathbf{q}_1$, because this triangle is acute-angled with the acute angle at the vertex, where the deuteron cluster is placed. From the viewpoint of hyperspherical variables, this corresponds to the significant mean value of angle β. We note the observed interesting situation concerning the root-mean-square radii of the states 1^+. The state with a higher energy has a less root-mean-square radius. This is quite possible in a three-cluster system, because the toughnesses of its oscillations along the directions set by the vectors $\mathbf{q}_1$ and $\mathbf{q}_2$ can be very different. The triangle representing the mutual position of clusters in the 2^+-state is obtuse-angled. It has a comparatively small height, but the elongated base. This allows us to assume that the formation of the wave function of the 2^+-state involves significantly the wave functions with $n_2 > 4$, i.e., $n_2 = 6, 8, \ldots$. Apparently, just this point ensures the relatively large value of root-mean-square radius of the nucleus in the 2^+-state.

It is of interest to determine the oscillator shells, whose functions contribute most essentially to the wave functions of states of the spectrum under study. This situation is illustrated by Fig. 6, where we present the total weights of functions of each of the shells, W_{sh}, depending on some number N_{sh} connected with the principal oscillator quantum number by the relation $N = 2N_{\text{sh}} + N_{\min}$. Here, $N_{\min} = 6$ for the positive-parity states of nucleus ^{10}B in correspondence with the filling rule in the oscillator model of shells, which is the limiting case of our approach for $N = N_{\min}$. The plots are artificially cut on the abscissa axes at the point corresponding to $N_{\text{sh}} = 14$, because the weights of each individual shell continuing further would be practically indistinguishable in the plot.

The results presented in Fig. 6 for the ground state indicate that a very large contribution ($\approx$70%) to its wave function comes namely from the states with $N = N_{\min} = 6$, which corresponds to the function of the oscillator shell model for its lowest shell occupation. This confirms the relative compactness of nucleus ^{10}B in its ground state as compared with other bound states, whose functions are spread to a greater degree over higher shells. Respectively, their clusterization is manifested more strongly, because the number of quanta of oscillator excitations is gathered due to the function of the relative motion of clusters. In

this case, we note that the results presented in Fig. 6 indicate, on the whole, the necessity to consider the functions of higher shells and, respectively, the clusterization in order to describe the properties of bound states of nucleus ^{10}B.

In order to demonstrate the significance of the spin-orbit forces for the formation of the proper mutual position of levels of the spectrum of bound states of nucleus ^{10}B once more, we considered the dependence of their energies on the intensity of the LS-forces. To this end, we multiply the amplitude of spin-orbit forces, which was recommended by the authors of the potential, by the factor $f_{\rm LS}$ varied in the process of calculations from 0.5 to 1.1. The results of such calculations are given in Fig. 7, where the dashed line shows the lowest breakup threshold $^6\mathrm{Li}+\alpha$ of the nucleus under study, from which all energies are reckoned. The dotted lines give the experimental energies of levels, and the solid lines show the theoretical values of energies of the states as functions of the quantity $f_{\rm LS}$.

We note at once that the energy of the first state $J^\pi = 1^+$ obtained by us is practically independent of the quantity $f_{\rm LS}$, since the results presented in Table 2 imply that this state is formed dominantly at the expense of the state $L^\pi = 0^+$. Respectively, the spin-orbit splitting itself is practically absent in this case. The completely different situation is observed for the state $J^\pi = 3^+$. As was mentioned above, it is mainly formed on the basis of the state $L^\pi = 2^+$. The state $L^\pi = 3^+$ and even some share of the state $L^\pi = 4^+$ are involved as well. Moreover, the proper difference of the energies of the first excited state and the ground state can be obtained already for a value of $f_{\rm LS}$, which exceeds slightly 1. The energies of the second 1^+ state and the 2^+ state decrease also, as $f_{\rm LS}$ increases, but they do not attain yet the experimental values.

Concluding this section, we present the results of calculations of the values of the spectroscopic factors SF_L for the virtual decay of nucleus ^{10}B into the three-cluster channel $\alpha+\alpha+d$. These factors are the normalizing coefficients of the wave functions of the relative motion of clusters $\Psi_L(\mathbf{q}_1, \mathbf{q}_2)$ under conditions that the total wave function of the state Ψ is normalized to 1. The spectroscopic factors SF_L are determined from the relation

$$|SF_L|^2 = \sum_{\overline{\nu}} |C_\nu|^2,$$

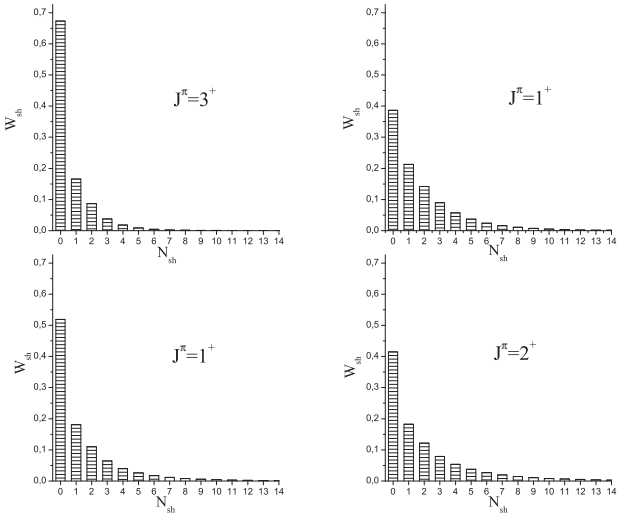

Fig. 6. Total weights $W_{\rm sh}$ of the functions of various oscillator shells in the wave functions of states of the discrete spectrum of nucleus ^{10}B as functions of the shell number $N_{\rm sh}$ (see the text)

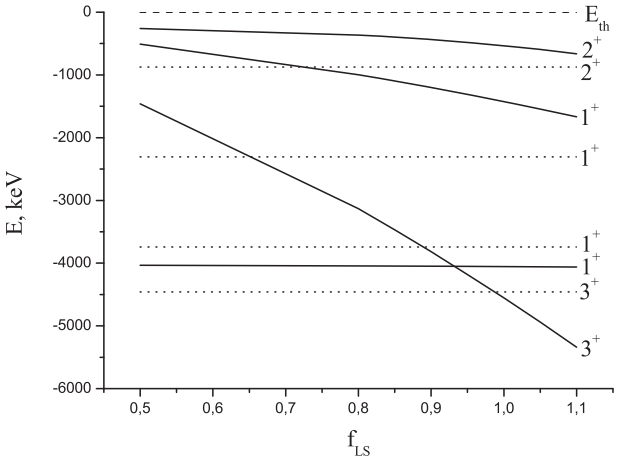

Fig. 7. Energies of bound states of nucleus ^{10}B versus the spin-orbit interaction intensity (see the text)

where the summation is carried out over all quantum numbers ν (see (7)) except for the orbital momentum. We note that the quantities SF_L can be useful to take approximately the Pauli principle into account, for example, by processing the experimental data in the frame of the potential model. To make it, one needs the results given in Tables 3 and 5, where the correspondence between the values of quantities $W(L)$ and SF_L should be noted. The large and small weights $W(L)$ correspond to the large and small val-

Table 5. **Spectroscopic factors SF_L and renormalized spectroscopic factors $\overline{SF}_L$ for the states with $L = J - 1$, $L = J$, and $L = J + 1$ in the three-particle channel $\alpha + \alpha + d$**

J^π	3^+	1^+	1^+	2^+
SF_{J-1}	0.863841	1.698726	0.000055	0.000378
SF_J	0.151081	0.001033	0.000142	1.352742
SF_{J+1}	0.016652	0.001012	1.971116	0.032111
$\overline{SF}_{J-1}$	1.033444	1.386661	14.339290	4.589016
$\overline{SF}_J$	1.010086	1.960402	3.467972	1.395862
$\overline{SF}_{J+1}$	1.145165	17.675393	1.265448	1.042262

ues of the spectroscopic factors, respectively, for each specific value of orbital momentum L. In order to more adequately describe the influence of the Pauli principle on each of the states with a given value of orbital momentum, we introduce the notion of the renormalized spectroscopic factor, which is connected with the traditional definition by the relation $\overline{SF}_L = SF_L/W(L)$. This definition of the spectroscopic factor implies that the component, which is characterized by the orbital momentum L and the spin S, of the wave function with the total angular momentum J, is normalized to 1. Such definition of the spectroscopic factors reflects more adequately, in our opinion, the influence of the Pauli principle on the function of the relative motion of clusters. In this case, the values of $\overline{SF}_L$ become much more larger than SF_L. It seems to us that this fact allows one to say, in some cases, about the states superallowed by the Pauli principle, for which $\overline{SF}_L$ is much more than 1. It is worth noting that the renormalization of the spectroscopic factors reveals no almost forbidden states, for which $\overline{SF}_L \ll 1$. The results of calculations of the quantities SF_L and $\overline{SF}_L$ with the collection of input parameters C3 are presented in Table 5.

4. Conclusions

The spectrum of bound states of nucleus ^{10}B is studied in the frame of a three-cluster microscopic model. The nucleus has been modeled by the three-cluster configuration $\alpha + \alpha + d$. The interaction of the clusters is given by a semirealistic nucleon-nucleon potential known as the Minnesota potential in the literature. We have studied how the density distribution of nucleons in the clusters α and d affects the spectrum of a compound-nucleus. The variation of the density distribution of nucleons was carried out due to the variation of the oscillator length. The effects of the spin-orbit interaction of nucleons on the structure of bound states are studied in detail. It is shown that the spin-orbit interaction affects essentially the spectrum of bound states and, depending on the intensity, can strongly change the mutual position of the levels of nucleus ^{10}B.

1. E. Caurier, P. Navrátil, W.E. Ormand, and J.P. Vary, Phys. Rev. C **66**, 024314 (2002).
2. P. Navrátil and W.E. Ormand, Phys. Rev. Lett. **88**, 152502 (2002).
3. P. Navrátil and and W. Ormand, Phys. Rev. **68**, 034305 (2003).
4. P. Navrátil and E. Caurier, Phys. Rev. C **69**, 014311 (2004).
5. E.C. Simpson, P. Navrátil, R. Roth, and J.A. Tostevin, Phys. Rev. C **86**, 054609 (2012).
6. P. Navrátil, V.G. Gueorguiev, J.P. Vary, W.E. Ormand, and A. Nogga, Phys. Rev. Lett. **99**, 042501 (2007).
7. A.M. Shirokov, J.P. Vary, A.I. Mazur, and T.A. Weber, Phys. Lett. B **644**, 33 (2007).
8. S. Pieper, C. Varga, and R.B. Wiringa, Phys. Rev. C **66**, 044310 (2002).
9. Y. Fujiwara and Y.C. Tang, Prog. Theor. Phys. **93**, 357 (1995).
10. D.R. Thompson, M. LeMere, and Y.C. Tang, Nucl. Phys. A **286**, 53 (1977).
11. H. Nishioka, J. Phys. G: Nucl. Part. Phys. **10**, 1713 (1984).
12. V.S. Vasilevsky, A.V. Nesterov, F. Arickx, and J. Broeckhove, Phys. Rev. C **61**, 034606 (2001).
13. A.V. Nesterov, F. Arickx, J. Broeckhove, and V.S. Vasilevsky, Phys. Part. Nucl. **41**, 716 (2010).
14. F.G. Lepekhin and B.B. Simonov, Yad. Fiz. **68**, No. 12, 1 (2005).
15. I. Reichstein and Y.C. Tang, Nucl. Phys. A **158**, 529 (1970).
16. K. Wildermuth and Y.C. Tang, *A Unified Theory of the Nucleus* (Acad. Press, New York, 1977).
17. E.J. Heller and H.A. Yamani, Phys. Rev. A **9**, 1201 (1974).
18. H.A. Yamani and L. Fishman, J. Math. Phys. **16**, 410 (1975).
19. V.S. Vasilevsky, A.V. Nesterov, F. Arickx, and P.V. Leuven, Yad. Fiz. **60**, 413 (1997).
20. Yu.A. Simonov, Yad. Fiz. **3**, 630 (1966).
21. A.M. Badalyan and Yu.A. Simonov, Yad. Fiz. **3**, 1032 (1966).

22. A.V. Nesterov, Yad. Fiz. **56**, 35 (1993).
23. G.F. Filippov and I.P. Okhrimenko, Yad. Fiz. **32**, 932 (1980).
24. G.F. Filippov, Yad. Fiz. **33**, 928 (1981).
25. G.F. Filippov, V.S. Vasilevsky, and L.L. Chopovskii, Fiz. Elem. Chast. At. Yadr. **15**, 1338 (1984).
26. T.Ya. Mikhelashvili, Yu.F. Smirnov, and A.M. Shirokov, Yad. Fiz. **48**, 969 (1988).
27. V.S. Vasilevsky and F. Arickx, Phys. Rev. A **55**, 265 (1997).
28. D.R. Tilley, J.H. Kelley, J.L. Godwin, D.J. Millener, J.E. Purcell, C.G. Sheu, and H.R. Weller, Nucl. Phys. A **745**, 155 (2004).
29. A. Ozawa, I. Tanihata, T. Kobayashi, Y. Sugihara, O. Yamakawa, K. Omata, K. Sugimoto, D. Olson, W. Christie, and H. Wieman, Nucl. Rhys. A **608**, 63 (1996).

Received 09.08.14

О.В. Нестеров,
В.С. Василевський, Т.П. Коваленко

СПЕКТР ЗВ'ЯЗАНИХ СТАНІВ ЯДРА ^{10}B
У ТРИКЛАСТЕРНІЙ МІКРОСКОПІЧНІЙ МОДЕЛІ

Р е з ю м е

У рамках мікроскопічної моделі – трикластерного варіанта Алгебраїчної Версії Методу Резонуючих Груп – розглянуто спектр зв'язаних станів ядра ^{10}B з $T = 0$. У ролі нуклон-нуклонного потенціалу використовувався напівреалістичний потенціал, що містить в собі центральну та спін-орбітальну компоненти. Точно врахована кулонівська взаємодія між протонами. Отримано правильний порядок рівнів у спектрі, що досліджується, розумне збігання з експериментальними даними по їх розміщенню відносно найнижчого порога розпаду ядра. Детально досліджено роль спін-орбітальної взаємодії у формуванні спектра зв'язаних станів ядра ^{10}B.